

Enhanced Carrier Lifetimes and Suppression of Midgap States in GaAs at a Magnetic Metal Interface

B. T. Jonker, O. J. Glebocki, R. T. Holm, and R. J. Wagner

Naval Research Laboratory, Washington, D.C. 20375-5343

(Received 10 July 1997)

We report the first measurement of room temperature carrier lifetimes at a magnetic metal–semiconductor interface, Fe/GaAs(001)-(2 × 4). The lifetimes are significantly *enhanced* relative to uncoated or sulfur-passivated surfaces, or the Al/GaAs(001)-(2 × 4) interface. These enhanced lifetimes correlate with a corresponding decrease in the density of midgap states which otherwise dominate the character of the GaAs(001) surface. The epitaxial Fe film provides both a ferromagnetic contact and a superior surface-passivating layer which does not pin the Fermi energy. [S0031-9007(97)04694-2]

PACS numbers: 73.20.-r, 73.61.Ey, 78.66.-w, 85.70.Yv

Magnetic metal–semiconductor heterostructures form the basis for an emerging class of devices which derive their utility from the combination of the magnetic and electronic properties of the individual material constituents [1–3]. Monsma *et al.* [2] recently fabricated a Si metal-based transistor utilizing a (Co/Cu) spin-valve multilayer as the base. The change in resistance of the base with applied magnetic field due to the spin-valve effect controlled the hot electron transport between the Schottky barrier emitter and collector. Datta and Das [1] proposed that a spin-polarized mode of operation could be realized in a III-V based field effect transistor (FET) by utilizing a ferromagnetic metal as the source and drain contacts, and modeled the response of the device in terms of spin-polarized transport and carrier spin precession in the high mobility two-dimensional electron gas channel.

The high mobility and optical properties inherent to III-V semiconductors make them especially attractive as a foundation for hybrid devices utilizing ferromagnetic layers in intimate contact with the semiconductor. However, many III-V materials are notoriously sensitive to surface/interface effects and the formation of midgap states which result in high surface recombination velocities, decreased carrier lifetimes, and Fermi level pinning [4,5]. A great effort has been made to develop procedures which passivate the exposed surfaces of III-V materials, most notably GaAs, with some success [6–8].

In this Letter, we report the first measurement of room temperature carrier lifetimes at a magnetic metal–semiconductor interface, Fe/GaAs(001)-(2 × 4). We find that the lifetimes are significantly *enhanced* relative to other surface terminations, and that this enhancement correlates with a significant *decrease* in the density of midgap states, which otherwise dominate the character of the GaAs(001) surface. We demonstrate that the epitaxial Fe film provides a ferromagnetic contact, suppresses midgap state formation, and does not pin the Fermi energy. These results have significant implications for the realization of magnetic metal–semiconductor spin transport devices. Recent calculations have shown that such states provide

a very efficient mechanism for spin relaxation at the GaAs surface/interface [9]. These states are a serious impediment to successful operation of spin-dependent metal–semiconductor tunnel junctions [9] and spin-polarized scanning tunneling microscopes which employ a GaAs tip [10]. The ability to suppress interface states also has implications for conventional III-V devices, such as GaAs-based FETs. Interface states at the metal Schottky gate junction reduce the device gain, increase the threshold voltage, and result in increased gate leakage current [11]. Gate leakage current results in increased power consumption and reduced noise margins in circuits [12].

The samples were grown in a multichamber molecular beam epitaxy (MBE) facility on n^+ -GaAs(001) wafers. They consisted of an n^+ -doped buffer layer followed by a 1000–1500 Å undoped GaAs spacer layer. The growth was terminated using a flux sequence [13] to produce a well ordered 2 × 4 As-dimer terminated surface reconstruction [14]. These surfaces exhibited a high degree of atomic order as confirmed by both scanning tunneling microscopy [15] and reflection high energy electron diffraction (RHEED), with average terrace widths of 0.25–0.5 μm. The sample was then transferred in ultrahigh vacuum (UHV) to a second MBE chamber, where Fe was deposited from a Knudsen cell-type source at a growth rate of ~3 Å/min and a substrate temperature of 175 °C, resulting in single crystal growth of a continuous 50 Å α -Fe(001) film whose crystallographic axes are aligned with those of the substrate. Such films exhibit room temperature ferromagnetism for thicknesses ≥ 9 Å [13]. After cooling the sample to slightly below room temperature, a 50 Å gold film was deposited to prevent oxidation of the Fe surface.

Photoreflectance (PR) spectroscopy was used to measure the Schottky barrier height and semiconductor carrier lifetimes in the interfacial region. These values were confirmed by electroreflectance (ER) spectroscopy, which was also used to assess Fermi level pinning on the metal coated samples. PR is commonly used to determine the electrical properties of a semiconductor surface or interface

[16–18] or the efficacy of III-V surface passivation procedures [8,16,19]. Redistribution of charge at an interface produces an electric field across a depleted region, resulting in field dependent oscillations in the optical constants at photon energies above the band gap known as Franz-Keldysh oscillations (FKOs) [17]. For the case of a uniform electric field and a small modulation, the differential reflectance signal, $\Delta R/R$, may be asymptotically written as [17]

$$E^2(E - E_g)^{-1/2} \frac{\Delta R}{R} \sim \Delta V \cos \left[\frac{4}{3} \left(\frac{E - E_g}{\hbar\theta} \right)^{3/2} + \phi \right] \times \exp \left[-2\Gamma \frac{(E - E_g)^{1/2}}{(\hbar\theta)^{3/2}} \right], \quad (1)$$

where E is the photon energy, E_g is the energy gap, ϕ is a phase factor, Γ is the reduced interband lifetime broadening parameter, and $\hbar\theta$ is the electro-optic energy. ΔV is the modulation voltage in the region of the electric field produced either by the pump laser in PR or by an applied ac bias in ER. The quantity $\hbar\theta$ is related to the electric field F and the reduced interband effective mass along the direction of the electric field, $\mu_{\parallel} = [(\mu_e^{-1} + \mu_h^{-1})^{-1}]$, through $\hbar\theta = (e^2 F^2 \hbar^2 / 2\mu_{\parallel})^{1/3}$.

As can be seen from Eq. (1), the sinusoidal FKOs are damped by an exponential envelope. The period of the oscillation is determined by the magnitude of the electric field, and the exponential damping is determined by the electric field and lifetime broadening Γ from which the reduced carrier lifetime is derived, $\tau = \hbar/\Gamma$ [17].

In the samples studied, the relative positions of the conduction band and Fermi energy (E_F) are established on either side of the undoped spacer by the n^+ doping and the surface (Schottky) barrier, respectively. This forms a capacitorlike structure with a constant electric field F across the known thickness d of the undoped spacer [20]. The measured surface barrier height is given approximately by $V_B \approx F^* d$ [21]. For uncoated samples, this value must be corrected for the surface photovoltage V_P to yield the true surface barrier $V_S = V_B + V_P$. The value of V_P at 300 K was found to be 100 meV from temperature dependent measurements, in agreement with previous results [22]. The metal coated samples exhibited negligible surface photovoltages.

The PR data were obtained at room temperature using a typical modulated reflectance apparatus [16,18] in which the 543 nm line of a He-Ne laser chopped at ~ 400 Hz was used as the modulation beam. In addition to the Fe contact samples, three other types of samples were grown in an identical manner and studied for comparison. An uncoated sample which was simply removed from the MBE system and exposed to atmosphere following GaAs growth and (2×4) -As surface termination was used as one reference sample, since the oxide/GaAs interface has been well characterized in the past [21]. This same sample was then

sulfur passivated using the wet chemical $(\text{NH}_4)_2\text{S}$ -based procedure [23], which is one of the more successful GaAs passivation procedures to date [6,7,19,24]. Finally, since the Al/GaAs interface has also been widely studied, an Al contact sample was prepared by cooling the sample in UHV to room temperature after GaAs growth, returning it to the III-V growth chamber, and depositing a 100 Å single crystal Al(001) film. This sample was also coated with Au.

The PR data are summarized in Fig. 1. The signal in phase with the modulating laser beam is shown as a solid line, while the dotted line shows the quadrature signal, which derives from midgap or defect states at the surface/interface. The FKO period (electric field) is approximately the same for each spectrum due to the different spacer layer thicknesses used, so that the obvious differences in FKO damping are due primarily to differences in carrier lifetimes.

The damping of the FKOs and the amplitude of the quadrature signal both vary dramatically for the four terminations of the GaAs-(2×4) surface, reflecting the strong influence of the interface. In the reference native oxide sample [Fig. 1(a)], the oscillations are well formed but strongly damped and extinguished by 1.75 eV. The period of the oscillations corresponds to a measured surface barrier height $V_B = 0.62$ eV, and a corrected value $V_S = 0.72$ eV. This value agrees well with that expected from the well-known pinning of E_F at midgap which accompanies the native surface oxide [21]. The stable oxide has been shown to be Ga_2O_3 , whose formation leads to the release of As [25]. Excess As at the interface pins E_F at midgap [22,26,27]. The very large quadrature signal confirms a high midgap state density. The strong damping of the FKOs can be understood in the context of these midgap states which act as centers for fast nonradiative recombination or scattering, resulting in a significant decrease in carrier lifetimes [16]. The lack of a benign native oxide has long been recognized as a significant shortcoming of GaAs-based device technology.

The PR spectrum obtained from this same sample immediately after sulfur passivation [Fig. 1(b)] exhibits a significant increase in the ratio of the in-phase to quadrature signals, but the FKOs are again strongly damped and the quadrature signal remains large. Although the midgap state density appears reduced due to this widely used passivation procedure, it still dominates the character of the interface. Similar comments apply to the Al/GaAs-(2×4) spectrum [Fig. 1(c)]—the FKOs are strongly damped and the quadrature signal remains large.

In contrast to the reference spectra, the FKOs in the Fe/GaAs-(2×4) spectrum [Fig. 1(d)] are much more pronounced and exhibit much less damping, extending to 2 eV. The significant reduction in damping indicates a substantial *increase* in carrier lifetimes. This is attributed to a suppression of midgap state formation, as indicated by the absence of a quadrature signal. These

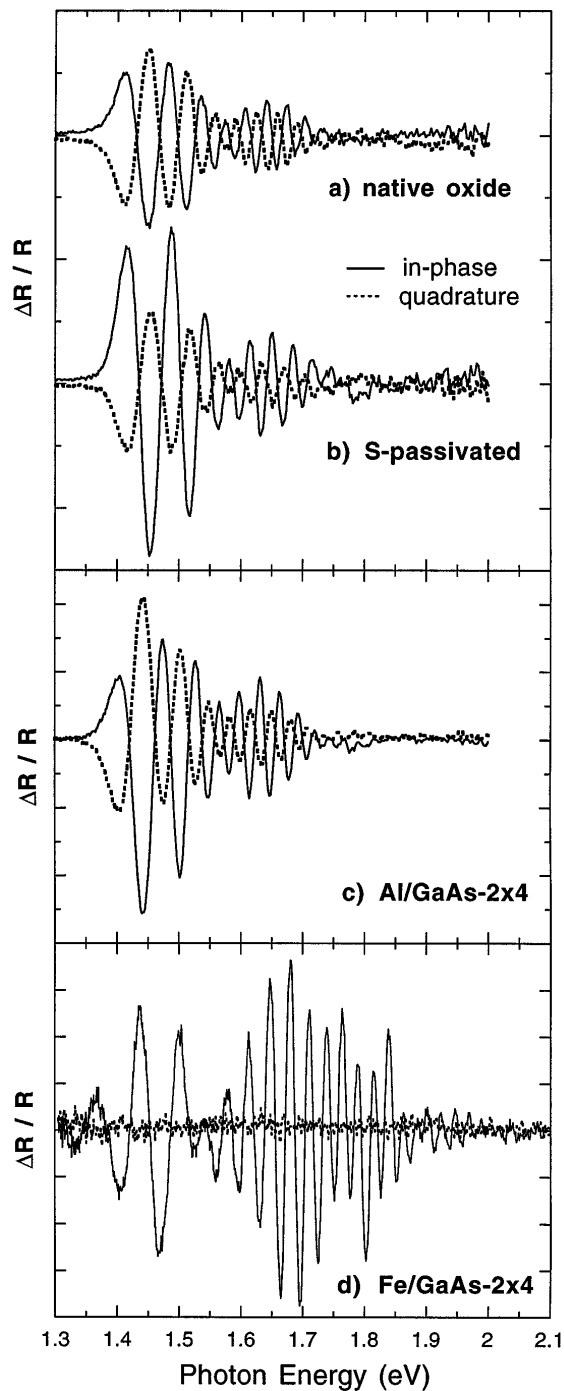


FIG. 1. 300 K PR spectra for (a) native oxide reference sample, $F = 58$ kV/cm; (b) same sample following sulfur passivation, $F = 61$ kV/cm; (c) Al/GaAs-(2×4) sample, $F = 55$ kV/cm, and (d) Fe/GaAs-(2×4) sample, $F = 60$ kV/cm. The thickness of the undoped spacer is 1070 Å for (a)–(c), and 1500 Å for (d).

data are representative of those obtained from four separate Fe/GaAs growth runs after optimization of growth conditions [13,15]. The period of the oscillations yields a surface (Schottky) barrier $V_S = V_B = 0.90$ eV, significantly higher than that of the reference samples, again indicating a

substantial reduction in the density of midgap states which would otherwise pin E_F and produce a lower barrier.

The reduction in midgap states can be further assessed by applying a variable dc bias voltage across the structure to forward or reverse bias the Schottky barrier. This effectively sweeps the semiconductor Fermi energy through the band gap at the interface (see insets in Fig. 2), and should result in a linear dependence of the resultant electric field on applied bias in the absence of interface states which would otherwise pin E_F . Deviations from linearity indicate Fermi level pinning. These data are plotted in Fig. 2 and were obtained by superimposing a small ac voltage on the dc bias for lock-in detection of the reflectance signal (ER) [18]. We find a linear dependence for applied biases of -0.6 V (reverse) to $+0.6$ V (forward), demonstrating that E_F can be moved freely from the valence band edge to just below the conduction band, respectively. At zero bias, E_F lies 0.52 eV above the valence band maximum. Under forward bias, the electric field in the undoped spacer is reduced as the conduction band is forced nearly flat, and the sample becomes highly conductive at $+0.6$ V, limiting the maximum forward bias voltage which could be applied. In contrast, similar data obtained for the oxide sample with a metal film surface contact (Pt) show pronounced deviation from linearity, saturating under forward bias due to midgap pinning. The Al-(2×4) sample showed no dc bias dependence, attributed to the high midgap state density as indicated by the large quadrature signal [Fig. 1(c)].

Quantitative values for the carrier lifetimes near the interface may be obtained by analyzing the data using Eq. (1), with the carrier lifetime as the principal fitting parameter. The model takes into account transitions from both light and heavy holes (light/heavy intensity fixed at 0.33 per their transition matrix elements); the interference

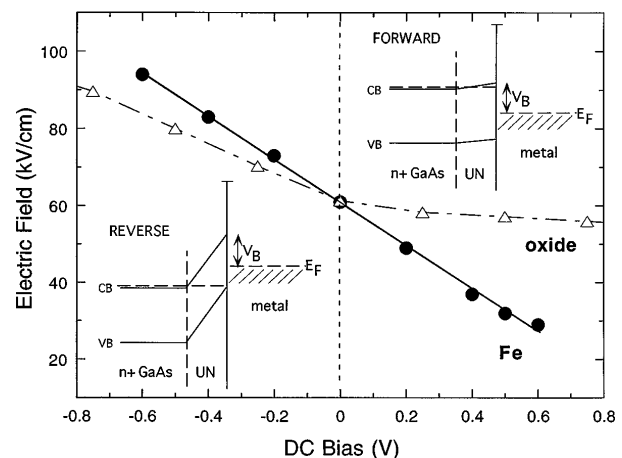


FIG. 2. Dependence of the electric field across the undoped GaAs spacer on the applied dc bias as obtained from ER spectra (300 K) for the Fe-(2×4) sample of Fig. 1(d) (solid circles, least-squares-fit line) and for a Pt/oxide-(2×4) sample (open triangles—these data have been shifted vertically by $+30$ kV/cm to coincide with the Fe data at zero bias). Insets show band diagram under forward and reverse bias conditions.

between these contributions produces the beating observed in the data. Quantitative fits to the spectra for the oxide, sulfur-passivated, and Al-coated samples (which exhibited strong damping and large quadrature signals) provide room temperature carrier lifetimes $\tau \approx 30$ fs. In contrast, the fits for the Fe-(2×4) samples yield a carrier lifetime of ~ 90 fs, a factor of 3 longer. The marked difference between these lifetimes can be explained by invoking a coupling of the bulk carrier wave functions to the midgap states localized at the semiconductor interface which provide a decay channel for the photoexcited electron-hole pairs. For the Fe/GaAs-(2×4) sample, there are few such states at the Fe/GaAs interface, and this decay channel is quenched, as manifested by the lack of a quadrature signal and an increase in carrier lifetime.

We do not believe that the ferromagnetic character *per se* of the Fe is critical to the observed suppression of midgap states. The atomic structure of the Fe/GaAs interface, however, offers some insight into the possible mechanisms responsible for suppressing these states. Previous work has shown that the growth of Fe on the GaAs(001)-(2×4) surface proceeds with the Fe displacing the first 0.5 monolayer (ML) of As (surface dimers) and the subsequent ML of Ga to form an Fe-As bonded interface, with a strong tendency for the liberated As to surface segregate [13]. This effectively transports the liberated As away from the interface, reducing the probability for the formation of As_{Ga} defects [26] or other As-related states [22], and results in an interface with an Fe-As bonding which we propose satisfies the two broken bonds per As atom, reducing the probability for the formation of defect states related to As dangling bonds. At least two Fe-As bonding geometries are suggested by the Fe:As interface stoichiometry of 2:1 [28] and the relative stability of the Fe_xAs_y compounds [29]. The stoichiometry suggests the formation of Fe_2As , one of the more stable compounds in the binary phase diagram. However, this would require substantial changes in the As bond angles. A more appealing bond configuration would result if we assume that half of the atoms in the first Fe ML substitutionally replace the first Ga ML, directly bonding to the As to form FeAs, which is slightly more stable than Fe_2As [29]. This has the advantage of minimally perturbing the As bond angle, since it requires no azimuthal bond rotation, while the polar angle energy minimum can be obtained by simple adjustment of the Fe to As plane spacing. The remaining half ML of Fe would be accommodated in sites above the underlying Ga atoms to form a square Fe surface net and an ideal atomic template for subsequent growth of the bcc Fe(001) film, rapidly transitioning the zinc blende GaAs structure to that of bcc Fe. We note that the Fe atoms in this first monolayer occupy two inequivalent sites, which is likely to produce a corrugation of the surface along both $[110]$ and $[\bar{1}10]$. Such a corrugation is consistent with the 2×2 reconstruction observed with RHEED during the early stages of growth.

In summary, we have found that an epitaxial Fe film on GaAs(001)-(2×4) suppresses the formation of midgap states which otherwise dominate the character of the GaAs surface, resulting in enhanced carrier lifetimes and unpinning E_F . These results have significant implications for magnetic metal–semiconductor spin transport structures, as well as conventional III-V devices, where the deleterious effects of interface states are well documented.

This work was supported by Office of Naval Research Contract No. N00014-97-WX20432.

-
- [1] S. Datta and B. Das, *Appl. Phys. Lett.* **56**, 665 (1990).
 - [2] D. J. Monsma *et al.*, *Phys. Rev. Lett.* **74**, 5260 (1995).
 - [3] G. A. Prinz, *Phys. Today* **48**, 58 (1995).
 - [4] W. E. Spicer *et al.*, *J. Vac. Sci. Technol.* **16**, 1422 (1979).
 - [5] S. Tiwari, *Compound Semiconductor Device Physics* (Academic, San Diego, 1992).
 - [6] C. J. Sandroff *et al.*, *J. Appl. Phys.* **67**, 586 (1990).
 - [7] S. Belkouch *et al.*, *Solid State Electron.* **39**, 507 (1996).
 - [8] M. Passlack *et al.*, *Appl. Surf. Sci.* **104/105**, 441 (1996).
 - [9] M. W. J. Prins *et al.*, *J. Phys. Condens. Matter* **7**, 9447 (1995), and references therein.
 - [10] R. Laiho and H. J. Reittu, *J. Phys. Condens. Matter* **9**, 5697 (1997).
 - [11] M. M. Ahmed, H. Ahmed, and P. H. Ladbrooke, *J. Vac. Sci. Technol. B* **13**, 1519 (1995).
 - [12] M. Shur, *Physics of Semiconductor Devices* (Prentice-Hall, Englewood Cliffs, NJ, 1990), p. 406.
 - [13] E. Kneedler *et al.*, *J. Vac. Sci. Technol. B* **14**, 3193 (1996); E. Kneedler and B. T. Jonker, *J. Appl. Phys.* **81**, 4463 (1997).
 - [14] J. Zhou *et al.*, *Appl. Phys. Lett.* **64**, 583 (1994).
 - [15] P. M. Thibado *et al.*, *Phys. Rev. B* **53**, R10481 (1996).
 - [16] O. J. Glembocki *et al.*, *Appl. Surf. Sci.* **63**, 143 (1993).
 - [17] D. E. Aspnes and A. A. Studna, *Phys. Rev. B* **7**, 4605 (1973); **10**, 4228 (1974).
 - [18] R. N. Battacharya *et al.*, *Phys. Rev. B* **37**, 4044 (1988); F. H. Pollak, *J. Vac. Sci. Technol. B* **11**, 1710 (1993).
 - [19] D. Paget *et al.*, *Phys. Rev. B* **53**, 4615 (1996).
 - [20] C. Van Hoof *et al.*, *Appl. Phys. Lett.* **54**, 608 (1989).
 - [21] X. Yin *et al.*, *J. Vac. Sci. Technol. A* **10**, 131 (1992).
 - [22] D. Yan *et al.*, *Phys. Rev. B* **52**, 4674 (1995).
 - [23] J. Fan *et al.*, *Jpn. J. Appl. Phys.* **27**, L1331 (1988); M. S. Carpenter *et al.*, *Appl. Phys. Lett.* **53**, 66 (1988); G. W. Anderson *et al.*, *Surf. Sci.* **346**, 145 (1996).
 - [24] M. Tanimoto *et al.*, *Jpn. J. Appl. Phys.* **33**, L279 (1994); M. Sugiyama *et al.*, *Jpn. J. Appl. Phys.* **34**, L1588 (1995).
 - [25] C. D. Thurmond *et al.*, *J. Electrochem. Soc.* **127**, 1366 (1980).
 - [26] W. E. Spicer *et al.*, *J. Vac. Sci. Technol. B* **6**, 1245 (1988).
 - [27] J. L. Freeouf and J. M. Woodall, *Appl. Phys. Lett.* **39**, 727 (1981).
 - [28] The atomic density of the bcc Fe(001) plane is approximately twice that of the bulk terminated GaAs(001) surface.
 - [29] M. Hansen, *Constitution of Binary Alloys* (McGraw-Hill, New York, 1958).